Design of experiments approach to luminescent CaMoO$_4$ by atomic layer deposition

(iD) **Julie Nitsche Kvalvik**, (iD) **Per-Anders Hansen, and** (iD) **Ola Nilsen**

COLLECTIONS

Paper published as part of the special topic on Atomic Layer Deposition (ALD)

View Online   Export Citation   CrossMark

ARTICLES YOU MAY BE INTERESTED IN

Design of experiments approach to luminescent CaMoO₄ by atomic layer deposition

Julie Nitsche Kvalvik, [iD] Per-Anders Hansen, [iD] and Ola Nilsen[a] [iD]

AFFILIATIONS

Centre for Materials Science and Nanotechnology, Department of Chemistry, University of Oslo, Postboks 1033, Blindern, 0315 Oslo, Norway

Note: This paper is part of the 2021 Special Topic Collection on Atomic Layer Deposition (ALD).
[a]**Electronic mail:** ola.nilsen@kjemi.uio.no

ABSTRACT

Atomic layer deposition (ALD) is evolving beyond binary compounds to complex oxides and doped structures, taking advantage of the nanometer precision ALD provides. In practice, the development of complex ALD-processes usually means performing many ALD-runs, as success at first attempt is unlikely. One factor at a time methods, where only one factor is altered and the rest are kept constant, are most often chosen due to their intuitive communication of control. However, they do have several drawbacks, being slow, neglecting secondary effects, and are usually not randomized—meaning that errors that arise over time can easily be overlooked. We here dig into our statistical toolbox and show how design of experiments (DoE) can be used to efficiently develop an ALD-process to deposit crystalline, luminescent CaMoO₄—a proposed material for optoelectronic applications, like light emitting diodes or as a host for solar down-converters. Using DoE enables screening for a wider range of deposition temperatures, pulsed composition, and annealing parameters, by only performing nine ALD-runs in our case. We moreover look into how these parameters affect crystallinity, composition, and the photoluminescence properties and use DoE to show which factors have the greatest effects on these properties. The work also lays out the basic theory of the DoE-field and how to implement DoE in developing ALD-processes, in general, to ease the usage of DoE for the ALD-community.

I. INTRODUCTION

Complex oxides are gaining importance in numerous fields from luminescence,[1,2] catalysis, and enabling oxide based electronics.[3,4] However, synthesis of such materials adds a level of complexity. This is particularly true for deposition by atomic layer deposition (ALD), where there is not necessarily a direct correlation between the pulsed and deposited compositions.[4] Also, optimizing the deposition temperature can be challenging. The ideal starting scenario, if the aim is to develop a novel ternary ALD-process, is that their binary processes have overlapping temperature ranges where they exhibit ALD-growth (ALD-windows). This is not a strict criterion, however, as ALD-windows do change when binary systems are used in combination for ternary or even quaternary processes.[5]

Traditionally, new complex ALD processes have been developed using one factor at a time (OFAT) methods.[6] This means that, for example, the deposition temperature has been altered stepwise, while the other parameters, for example, the pulsing ratio between the components, pulsing and purging times, etc., have been kept constant. Thus, OFAT approaches require a large number of experiments, as the various factors are probed sequentially. In addition, interaction effects may be overlooked, such as how the required pulsing times vary with the deposition temperature. Moreover, OFAT processes are not intrinsically randomized and do, therefore, not reveal errors that arise over time, like developing leaks or clogs. The well-trained experimentalist should of course know that the experiments should be randomized, but we often see that this is not the case in practice, particularly for exploratory experiments where the boundaries are not known in advance, such as temperature range, times, etc.

The weaknesses of OFAT methods can be overcome by performing screening and optimizing using a design of experiments (DoE) framework. DoE applies statistics not only when analyzing the measured data but also to set up the experiments themselves. By changing several factors at a time in a pre-determined and

randomized order, a maximum amount of information is retrieved from a given number of experiments. Since the order of the experiments is randomized, the residuals, namely, the difference between the obtained and predicted value, can be plotted as a function of time to reveal errors that arise over time.

The concept of DoE was first proposed in 1935.[7] Today, Plackett–Burman designs are widely used as screening designs for processes with many factors,[8] whereas various response surface methodologies (RSMs)[9] such as central composite designs (CCDs)[10] are used for optimizations. When using RSM, the existence of a response surface modeled with polynomials with at least two variables is postulated. A measured response for an ALD-system could, for example, be the growth per cycle (GPC). The variables used to model the response surface are termed input or predictor variables. The input variables represent the variables that can be changed between the experiments, such as the deposition temperature or pulse length in an ALD-experiment.

Considering what powerful and relatively easy to use tool DoE is, the extent it is being used in materials science today is surprisingly limited. This is probably related to that it requires some additional knowledge of statics beyond the basics. It also comes with the psychological barrier of giving a computer program the power of deciding your experiments. A program that on overall feels a bit like the black box we researchers typically do not like to relate to. However, in reality, it is still researcher's job to decide on the investigated experimental region and the data density and distribution within it, even when DoE is used. In fact, DoE forces the researcher to plan carefully in advance of performing the experimental series, which reduces the risk of failed experiments and, thus, time and resources.

DoE has been used in the development of electrospinning processes,[11] chemical vapor deposition of carbon nano-tubes,[12] and very recently in a work using synthesis of oleylamine-capped gold nanoparticles as a case study of how DoE can be implemented in nanoparticle synthesis.[13] However, using the DoE methodology is definitely the exception rather than the rule. There are a few examples of DoE being used in the ALD-community. Two factorial central composite designs have been used to map how the film thickness and annealing time of both amorphous TiO_2 (Ref. 14) and ZnO (Ref. 15) affect the optical properties. Moreover, DoE has been used to optimize the sheet resistance of TiN films deposited by plasma enhanced ALD using a full factorial DoE-experiment.[16] The input variables used there were the plasma duration, purge time, and the flows of N_2 and H_2.

We here show how DoE, more specifically a CCD-optimization, can be used to develop an ALD-process for the deposition of the ternary oxide $CaMoO_4$ and guide how similar ALD-challenges can be overcome by clever usage of DoE. $CaMoO_4$ shows interesting optical properties similar to other molybdates and tungstates with the tetragonal Scheelite-structure is proposed as a host material for down-conversion thin films for solar cells. $CaMoO_4$ absorbs UV-light well but is transparent for lower energy photons, while it is easily doped with various lanthanides, making this material a suitable host for down-converting thin films (see the supplementary material[44] for UV-VIS specter of $CaMoO_4$). An important aspect with $CaMoO_4$ and other scheelites is that their intervalence charge transfer states (IVCTs) are high as compared

to, for example, vanadates, tungstates, or niobates.[17–22] This is important for the proposed use as a host for down-conversion thin films since it makes it less likely that the host material itself will induce quenching of the excited lanthanides dopants through the IVCT state. However, present synthesis routes do not facilitate making sufficiently high-quality $CaMoO_4$ thin films,[23–27] especially for further doping of the host matrix. ALD is an ideal method for such tasks and making $CaMoO_4$ by ALD should be possible by combining known processes for the deposition of CaO (Ref. 28) and MoO_3.[29] Another argument for why ALD is particularly useful is that it enables control of where the lanthanide dopants are placed in the host matrix, which, in turn, affect the energy transfer and thus luminescence properties, if indeed used as a down-converter on a later stage.

28 shows that $Ca(thd)_2$ (thd = 2,2,6,6-tetramethyl-3,5-heptanedione) + O_3 process yields CaO when deposited at 350 °C, but $CaCO_3$ at 250 °C, also without a CO_2 pulse. In general, β-diketonates, such as $Ca(thd)_2$, are well suited as ALD-precursors, especially at higher deposition temperatures or in combination with O_3.[30] $Ca(thd)_2$ has also been used to deposit $La_{1−x}Ca_xMnO_3$.[5]

The Mo-precursor used, namely, $MoCl_4O$, is much less investigated as an ALD-precursor. The availability of Mo-precursors that both are able to sustain temperatures above 195 °C [adequate sublimation of $Ca(thd)_2$] and work with conventional thermal ALD is very limited. In fact, the only other known option is $(N^tBu)_2(NMe_2)_2Mo$[31] but requires heating and inert handling. $MoCl_4O$ was chosen based on our recent experience with its sufficient vapor pressure at room temperature and use as a precursor to form MoO_x, although in a selective area process.[29]

Here, the pulsing ratio between $Ca(thd)_2$ and $MoCl_4O$, the deposition temperature, the annealing temperature, and annealing time are used as input variables, and the composition measured by energy-dispersive x-ray spectroscopy (EDS), a Pawley-refined x-ray diffraction (XRD) signal of $CaMoO_4$, and photoluminescence (PL) intensity are used as modeled response variables. Through such an analysis, we find that luminescent $CaMoO_4$ thin films can be deposited by ALD at 350 °C using 29 pulsed % of Mo precursor versus Ca precursor and that longer annealing times increase the PL signal. We further comment on how this approach can be transferred to future mapping of complex compounds by ALD.

II. EXPERIMENT

Prior to performing the CCD-experiment, a few initial trials were performed to test if the combination of the binary processes could yield $CaMoO_4$ and to give hints on the span of the input parameters. In general, to start a DoE set without some initial information is not recommended, especially when optimizations are used, as they require a process that is already somewhat established. DoE is not a quick fix for not knowing your chemistry but a tool to tune your process. The initial trials revealed a few points that helped to provide the starting point for the CCD-series:

(i) Using a pulsing ratio of 1:1 with $[MoCl_4O + (H_2O + O_3)]$ versus $[Ca(thd)_2 + O_3]$, hereafter termed 1:1 of Mo:Ca, and depositing at 300 °C gave a huge surplus of molybdenum [about 80% Mo as measured by x-ray fluorescence (XRF)].

(ii)   Pulsing 1:1 of Mo:Ca did not give any XRD-peaks of CaMoO$_4$.

(iii) Annealing at 1000 °C for 1 h gave rise to unwanted Si–Mo phases.

(iv)   Although pulsing 1:2 or 1:3 of Mo:Ca gave a small surplus of calcium when deposited at 300 °C, it showed signs of CaMoO$_4$ in the diffractograms.

The last point in the list above attached weight to that the MoCl$_4$O + (H$_2$O + O$_3$) and Ca(thd)$_2$ + O$_3$ processes indeed could be combined to form CaMoO$_4$.

The thin films were deposited by ALD using a F-120 Sat reactor (ASM Microchemistry). Si(100) wafers with a 2 nm thick native oxide layer were used as substrates. The deposition temperature was an input variable in the experiment and ranged from 300 to 400 °C. We hoped that increasing the deposition temperature to 400 °C would aid crystallization during deposition. N$_2$ from gas cylinders (Praxair, 99.999%), passing through a Mykrolis purifier, was used as a purging gas with a flow rate of 300 cm^3 min^{-1}. A background pressure was maintained at 2.7 mbar. The depositions were carried out using the β-diketonate chelate Ca(thd)$_2$ (Strem, 97%) as the Ca-source, MoCl$_4$O (Sigma-Aldrich, 97%) as the Mo-source, O$_3$ as an O-source after the Ca(thd)$_2$ pulse, and distilled H$_2$O and O$_3$ pulsed simultaneously as the O-source after the MoCl$_4$O-pulse. O$_3$ was supplied from a In USA ozone generator (AC-2505), which delivers mass 15% O$_3$ in O$_2$, using O$_2$ from a gas cylinder (Praxair, 99.8%). Pulsing and purging times for the various precursors were chosen based on prior experience with deposition of MoO$_x$ (Ref. 29) and CaCO$_3$ (Ref. 28) on the same reactor and are given in Table I.

In this work, a face-centered CCD with four input variables (deposition temperature, pulsed % of Mo, annealing time, and annealing temperature) is used. Such a design with *three* input variables is visualized in Fig. 1. The star points are placed on the surfaces of the interaction cube where each direction represents the level of an input variable. The input variables are coded within this cube to range between −1 and 1, in order to be dimensionless and directly comparable with each other. For example, if the deposition temperature is varied between 200 and 300 °C, −1 is 200 °C, 0 is 250 °C, and 1 is 300 °C. The star points are placed a distance α from the center. The value of α should be chosen with care. It is typically settled after defining the factorial points, which define the range and also the center point. Note that 1 < α generates experiments outside the range of the factorial points. A small α gives a larger data density close to the center point. This is beneficial when convinced that the optimum is near the center. On the other hand, the explored region will be sma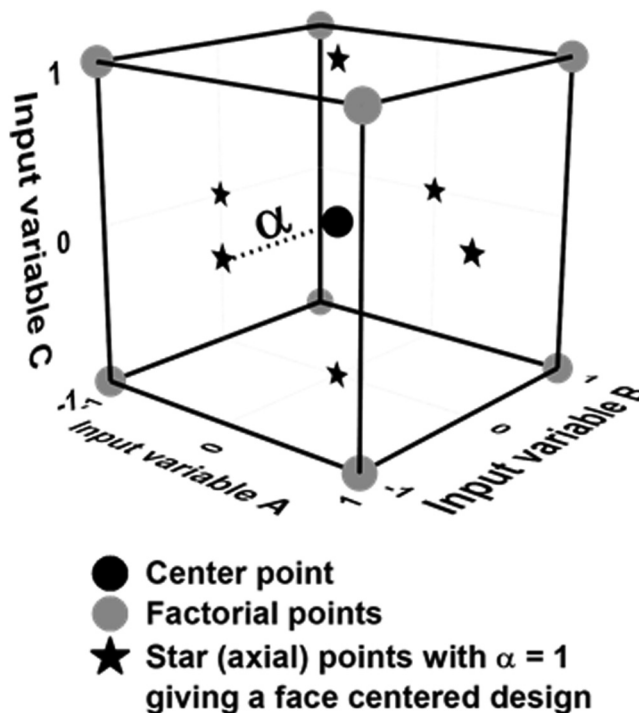ller and the data density in the periphery be poor when α is small. A face centered design (α = 1) as utilized here will not generate experiments outside the predefined ranges of the input variables. Moreover, batching is eased for face centered designs. The default value of α is usually $\sqrt{2}$, however, this may lead to experiments where α carry no physical meaning, like having a negative anneal time. The interested reader is referred to Ref. 32 for further information about CCD, where chapter 12 provides an excellent introduction to response surface methodology (RSM).

The pulsed composition of MoCl$_4$O + (O$_3$ + H$_2$O) relative to the total number of cation cycles was kept between 25% and 33%, as these compositions both showed signs of CaMoO$_4$ in the diffractograms. It is further referred to as pulsed % Mo. 29 pulsed % Mo was approximated with 5 cycles of MoCl$_4$O + (O$_3$ + H$_2$O) to 12 cycles of Ca(thd)$_2$ + O$_3$ with a pulsing sequence of Mo–Ca–Ca–Mo–Ca–Ca–Ca–Mo–Ca–Ca–Mo–Ca–Ca–Mo–Ca–Ca–Ca. The pulsed % Mo was also an input variable and varied according to the CCD setup. Some of the resulting films were annealed for improved crystallization and luminescence of CaMoO$_4$. The annealing time was either 15 or 30 min, and the annealing temperature was varied between 415 and 800 °C, both being input variables in the CCD setup. We chose 425 °C as the minimum annealing temperature, to span from just above the deposition temperature, and 800 °C as the maximum temperature, since it was significantly below 1000 °C, which led to formation of molybdenum

FIG. 1. Illustration of an interaction cube for a CCD with three input variables coded between −1 and 1. The design is face centered with the star points on the faces of the cube.

TABLE I. Standard pulsing and purging times for ALD synthesis of CaMoO$_4$.

Precursor	Pulse time (s)	Purge time (s)
MoCl$_4$O	3	3
H$_2$O + O$_3$	3	5
Ca(thd)$_2$	3	2
O$_3$	2	2

TABLE II. Overview of input variables with their ranges used in the experimental design.

Input variable	Minimum (coded −1)	Maximum (coded 1)
Deposition temperature (°C)	300	400
Pulsed % of Mo	25	33
Anneal temperature (°C)	425	800
Anneal time (min)	0	30

silicates in the initial studies. A MTI—UL Standard Compact RTP furnace utilizing halogen lamps was used for annealing. The samples were cooled rapidly after annealing. To save time and resources, the syntheses were performed in batches, as described in Table II of the supplementary material.[44] The setup of the experiments and statistical analysis were done using the MINITAB19 software with a face-centered central composite design. Table II gives an overview of the input variables used in the experimental design and their ranges. The full experimental setup as derived from MINITAB19 is given in Table I in the supplementary material.[44]

The selection of response variable(s) to study and how these should be characterized and digitized must be carefully considered prior to starting the investigations. It is all about what material and which properties are desired. If a clear goal is not defined, optimizing a process is futile. Two types of data can be analyzed with MINITAB19, both qualitative data (yes/no) and quantitative data. For the further quantitative statistical analysis, it is vital to have data that convey actual physical, comparable information.

To retrieve structural, compositional, and photoluminescence data of the samples, which were the three responses we desired to study, XRD, EDS, and PL analyses were done on the full set of samples. XRD was performed to investigate the structure of the obtained samples, using a Bruker D8 Discovery Diffractometer, with CuKα_1 radiation and a Ge(111) monochromator in a traditional Bragg–Brentano setup. In order to quantify the XRD data in a manner more suitable for MINITAB19, Pawley refinements were performed.[33] In this manner, potential overlapping peaks from undesired phases were accounted for. In opposition to Rietveld refinements, Pawley refinements can fit diffractograms showing oriented growth, which may occur for ALD-deposited films. The refinements were done using TOPAS.v5 and the data were fitted to COD No. 9009632. Integrated intensities for (011), (112), (013), and (004) peaks were retrieved and summed, prior to loading these data into MINITAB19 for further statistical analysis. EDS was performed using a HITACHI TM3000 scanning electron microscope equipped with a Quantax70 EDS unit. An acquisition time of 1 min was used. Prior to loading the data into MINITAB for further analysis, the content of Ca versus Mo in the samples was calculated. A higher value than 1.0 here, therefore, indicates a calcium surplus. The average of three measurements from different spots was used. The PL measurements were performed using a USB2000+ modular spectrometer from Ocean Optics with a 280 nm diode as the excitation source. All PL measurements were done in one session to make the data comparable. For the CCD analysis of the PL data, the integral between 450 and 850 nm is used. Selected samples were

also studied with atomic force microscopy (AFM) to get a measure of the roughness and topography. A Park Systems XE-70 AFM with a CONTSCR tip in a contact mode was used for this, and Gwyddion software was used to process the AFM micrographs. The film thicknesses and, thus, the GPC was measured by spectroscopic ellipsometry (SE) using a J. A. Woollam α-SE spectroscopic ellipsometer. The data were modeled with a Cauchy-function using the COMPLETEEASE software package. XRF was performed to probe for chlorine impurities stemming from the MoCl$_4$O-precursor and to verify the EDS-results, as XRF is considered more accurate but have stricter requirements on sample size, thus limiting our possibility to perform such analysis on the full set of samples. XRF was performed with a PANalytical Axios minerals max spectrometer equipped with OMNIAN and STRATOS softwares, and Omnian standards.

III. RESULTS AND DISCUSSION

A. Optimizing with design of experiments

All the experiments were carried out successfully as listed in Tables I–III in the supplementary material[44] and fitted to a response surface using MINITAB19. There were, however, gradients normal to the flow direction in the chamber for all the experiments yielding CaMoO$_4$. The films around 2 cm from the center of the reaction chamber were typically 50% thinner. Only samples that were centered in the reaction chamber were used for the further analysis and annealing experiments. The residuals for the various responses versus these response surfaces as a function of experiment order are given in Fig. 1 in the supplementary material.[44] As the goal of this work was to identify an ALD-route to obtain crystalline, luminescent CaMoO$_4$ thin films, MINITAB19 was used to optimize the process for two different cases.

(1) Maximize the XRD and PL signals and keep Ca:Mo closest possible to 1:1.
(2) Only maximize the PL signal.

The results of these calculations are given in Table III.

Pareto charts are typically shown when presenting DoE results, as they give an easy visualization of the effects of the various input factors,[34] here given in Fig. 2. Statistically valid effects within our desired confidence interval (95%) have values higher than 2.086 as given with the red dotted lines. For the crystallinity, the statistical analysis leaves no clear conclusions, as no terms have a statistically valid effect. That being said, the secondary effect between deposition temperature and annealing time, followed by

TABLE III. Optimization of the deposition process to maximize XRD and PL signals and keep Ca:Mo close to 1 (i) or only maximize PL signal (ii).

Process parameters	Optimized for case (i)	Optimized for case (ii)
Deposition temperature (°C)	340	349
Pulsed % Mo	30	29
Annealing temperature (°C)	686	626
Annealing time (min)	30	30
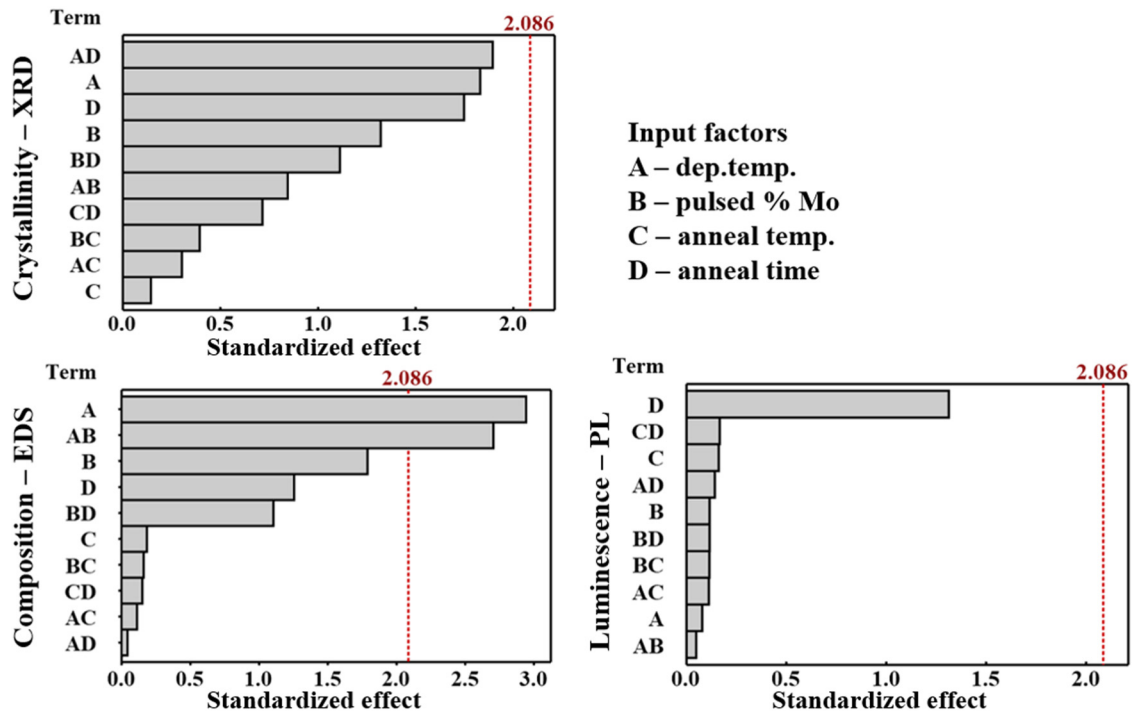
FIG. 2. Pareto charts showing the direct and secondary standardized effects of the input variables on the three responses. The dotted line at 2.086 denotes if the effects are indeed statistically significant or not. Standardized effects are unitless quantities.

these two factors alone, are the parameters closest to being significant. Surprisingly, the least significant effect is the annealing temperature, which seem to have a very limited effect on the crystallinity. This will be a topic in the discussions later. The only terms that show significance for the composition are the deposition temperature and the secondary effect between this and the pulsed percentage of Mo. The deposition temperature of any ALD process will, in turn, affect the packing density of the various precursors, both how many precursors that are available on the surface and their positions, which, in turn, affect how likely it is for $CaMoO_4$ to be deposited. Annealing, especially the annealing temperature, has a very limited effect on the composition, as expected. In like manner as with the crystallinity, no factors are statistically significant for the PL signal. However, the response is much higher for the annealing time than any of the other parameters.

Main effect plots, giving the average of all the measured responses for each level of the input variables, are also typically shown when presenting DoE data.[35] In this case, the main effect plots in Fig. 3, to a large extent paint the same picture as the optimization calculations in Table III for the ALD-deposition parameters. Both the PL and XRD signal maximize at the middle value for the pulsed % Mo (29%). Moreover, the EDS response is closest to 1 for this sample. Pulsing slightly
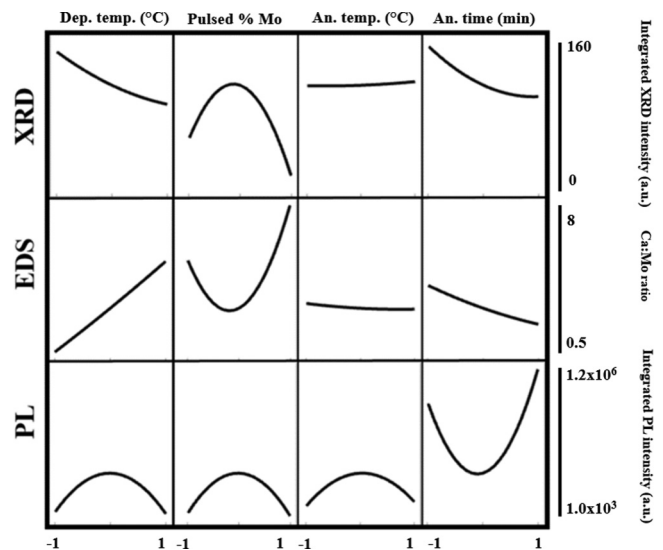
FIG. 3. Main effect plots showing mean values of all the measured responses for the various levels of the coded (−1 to 1) input parameters. The middle of each x axis represents coded value 0 for each input variable.

higher or lower content of Mo is according to this giving Ca-dominated thin films, more on this aspect in the discussions. For the deposition temperature, 350 °C seems to be a good compromise giving close to the correct stoichiometry, a high XRD-response and high PL-response.

Moreover, Fig. 3 shed light over the chosen annealing parameters. The composition seems nearly unaffected by annealing. The effect of annealing on the crystallinity is as seen in the Pareto charts also very limited, besides a slight decrease in XRD signal for the longer annealing times. Surprisingly, the PL values are higher for the samples that are not annealed than for the samples annealed for 15 min. We do, however, see the maximum PL values for samples that are annealed for 30 min. This suggests an ongoing crystallographic reorganization of the film where an intermediate microstructure is unfavorable for PL. The maximum mean PL values are found for an annealing temperature of 612.5 °C. All in all, the means of these experiments suggest that depositing at 350 °C with 29 pulsed % Mo, annealing at 612.5 °C for at least 30 min is a viable route to obtain crystalline, luminescent $CaMoO_4$ thin films by ALD.

B. Thin film growth and characterization

Figure 4 shows the growth rate per cycle (GPC) as a function of deposition temperature for three different pulsed % of Mo. Pulsing 25% or 33% of Mo have similar temperature dependencies on the GPCs with decreasing values from 300 to 350 °C before flattening out between 350 and 400 °C. For 29 pulsed % Mo, the GPC is increasing as a function of temperature between 300 and 400 °C. The GPC is 0.49 Å/cycle at 300 °C but is more than tripled at 400 °C where it is 1.75 Å/cycle. The differences in temperature dependencies of the growth rates for the various pulsed compositions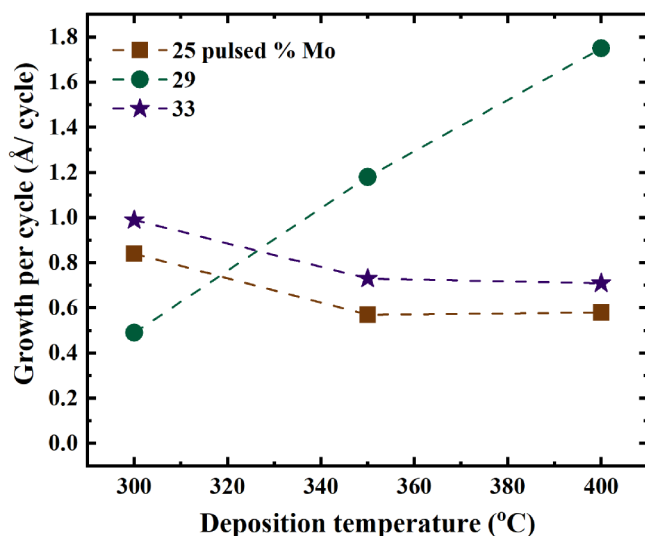 are probably related to which materials and phases are formed for each temperature. The samples found calcium-rich by EDS also had peaks from aragonite and calcite in their diffractograms. As the mean value plots of the EDS measurements in Fig. 3 suggest that samples deposited with both 25 and 33 pulsed % Mo are more calcium rich than the ones deposited with 29 pulsed % Mo. This indicates that the GPC of $CaMoO_4$ is increasing as a function of temperature for this system, whereas deposition of $CaCO_3$ shows the opposite tendency.

Figure 5 compares the XRD diffractograms obtained for films deposited by 29% pulsed Mo at various deposition temperatures. At 300 °C peaks from $CaMoO_3$, the 113-peak from calcite and a broad possible 104-peak from $CaMoO_4$ are found. At 350 °C, the $CaMoO_3$ peaks vanish but a sharp 104-calcite peak arise. Note that this 104-calcite peak is not seen for the samples deposited at 350 °C using 29 pulsed % Mo, that are also annealed, not consistent with an unaffected stoichiometry with annealing. At 400 °C, only peaks from $CaMoO_4$ are found. This is supported by the PL raw data given in Table I in the supplementary material,[44] as the sample deposited at 400 °C using 29% pulsed Mo is the most luminescent as deposited. It is, though, less luminescent than the samples deposited at 350 °C and annealed for 30 min.

Although the growth rate showed different temperature dependencies, there were several general trends for growth of these thin films, one being that the crystallite sizes ranged between 30 and 40 nm for the samples containing crystalline $CaMoO_4$ with a film thickness of ca. 120 nm. As many of the samples were similar with respect to both topography, photoluminescence, and crystallinity, PL, XRD, SEM, and AFM data for a selected sample are compiled in Fig. 6. The selected sample was deposited at 350 °C using 29 pulsed % Mo and was annealed at 612.5 °C for 15 min. It, thus,
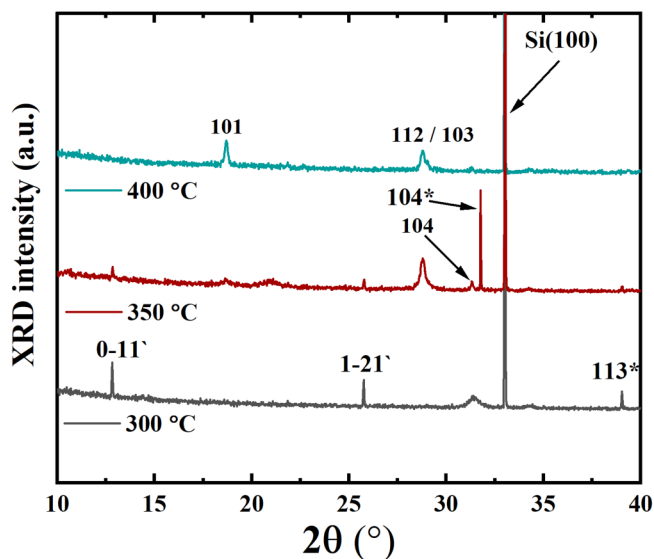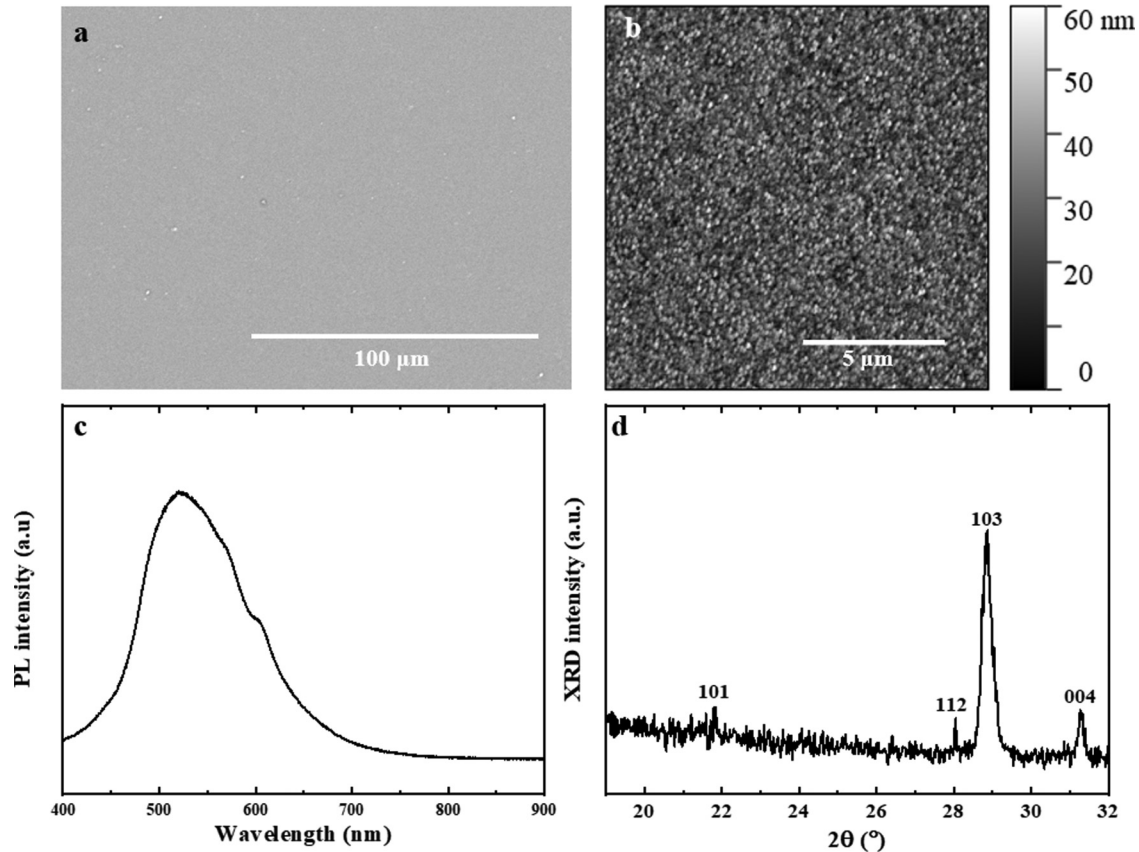

FIG. 4. GPC for $CaMoO_4$ for the various pulsed amounts of Mo vs Ca precursor as a function of deposition temperature.

FIG. 5. XRD diffractograms for samples deposited with 29 pulsed % Mo at various deposition temperatures. Indexes marked with * refers to calcite, ` refers to $CaMoO_3$, and no markings refers to the desired $CaMoO_4$ phase.

FIG. 6. SEM micrograph (a), AFM micrograph (b), PL spectrum (c), and XRD diffractogram (d) of a sample deposited at 350 °C using 29 pulsed % of Mo and annealed for 15 min at 612.5 °C. The film thickness was measured to be 114.4 nm by spectroscopic ellipsometry.

represents the center point of our imaginary interaction space in the CCD setup.

AFM was used to measure the roughness and topography of selected samples. The roughnesses together with relevant sample information are listed in Table IV. It reveals RMS roughnesses range between 8.9 and 20.0 nm for samples deposited at 350 °C using 29 pulsed % Mo. Annealing does not seem to affect the

roughness significantly, but the two samples with the lowest roughness are the ones annealed longest or at the highest temperature. Compared with the crystallite sizes retrieved from Pawley refinements, the RMS roughness is about half of the estimated crystallite size.

XRF analysis was performed on selected samples. Table V shows XRF data for a sample deposited at 350 °C using 29 pulsed % Mo. The measurement was performed prior to annealing. The chlorine content was below 1.5% in all measured samples. The XRF measurements all show a similar over-stoichiometry in this range for Mo, contrary to the EDS measurements.

TABLE IV. RMS roughness and relevant sample parameters for a selection of $CaMoO_4$ thin films deposited simultaneously at 350 °C using 29 pulsed % of Mo vs Ca but with different annealing parameters.

Film thickness (nm)	RMS roughness (nm)	Anneal time (min)	Anneal temperature (°C)
121.8	18.0	0	–
124.2	20.0	15	425
129.3	8.9	15	800
114.4	16.0	15	612.5
135.3	14.3	30	612.5

TABLE V. Mol. % of Mo, Ca, and Cl for a $CaMoO_4$ sample deposited at 350 °C using 29 pulsed % of Mo vs Ca measured by XRF prior to annealing.

Element	Mol. %
Mo	54.1
Ca	45.2
Cl	0.7

C. Discussion

Performing this CCD-experiment enabled us to find a synthesis route to fabricate photoluminescent, crystalline $CaMoO_4$ thin films by ALD—which was the main target of this work. Based on a few initial tests, we investigated a fairly narrow range in pulsed composition but a wider range of deposition temperatures and annealing conditions. An alternative approach to CCD could have been to perform an initial screening design, such as a wide range two-level Plackett–Burman design, especially of pulsed composition. In practice, this would have led to not performing the most successful experiments here, and may not have increased the knowledge of the system significantly. The initial tests proved to be a sufficient starting ground for this CCD-optimization, although the methodology was originally developed for a much simpler system where competitive products do not form to the same degree. Taking into account that the center point of the CCD-setup was replicated six times and that a few experiments had no annealing and, thus, were similar, a total of 21 different combinations of the four input factors have been tried. This was done using only nine ALD-runs and annealing in six batches. A significantly larger set of samples and experiments would have been required using the OFAT approach. More importantly, OFAT will in general not lead to the optimum condition if there is a correlation between the input parameters,[36] meaning that the optimum condition may not have been found at all if we had used OFAT here. We estimate that the number of ALD-runs would easily exceeded 20 for a process like this to be developed without DoE.

29 pulsed % Mo was the pulsed composition that yielded the most luminescent films and also the highest XRD-signal. Moreover, the temperature dependency was different for this pulsed composition than 25 or 33 pulsed % Mo, where 29 pulsed % Mo increase with temperature and the others decrease. This dependency with GPC, in combination with the gradients along the sides of the reaction chamber, suggests that the process is very sensitive toward the pulsed composition. We believe that the deposited composition is different on the sides of the reaction chamber due to fluid dynamics. The fact that the pulsing sequence for 29 pulsed % Mo actually consists of two Mo–Ca–Ca–Ca (= 25 pulsed % Mo) and three Mo–Ca–Ca (= 33 pulsed % Mo) units underlines this sensitivity further. We are surprised of this extreme sensitivity toward the pulsing composition, providing excess Ca on both sides of 29 pulsed % Mo. However, the randomized sequence of depositions moreover support that this extreme sensitivity toward pulsed composition is indeed a real effect. We expect that deviations from ideal composition will lead to formation of the slower growing $CaCO_3$, and that we grow $CaMoO_4$ in the center of the reaction chamber but more $CaCO_3$ to the sides. The GPC of $CaCO_3$ using $Ca(thd)_2$ and O_3 is reported as 0.45 Å/cycle at 300 °C and decreases to around 0.40 Å/cycle at 400 °C.[28] This decrease is less than what we see in the present dataset but may account for some of it.

We have recently reported the $MoCl_4O + (H_2O + O_3)$ process which grows selectively on LiF and conventional glass substrates[29] but show no signs of growth on $CaCO_3$ and Si(100) substrates among others. The MoO_x films deposited on LiF and glass had significant concentrations of Li^+ and Na^+, respectively, and we, therefore, believe that the growth of these films is limited by diffusion from the substrates. In the current work, calcium seems to also play a role since a high content of Mo was indeed possible, even though prior experiments has shown that a significant deposition of MoO_x was not possible on $CaCO_3$. This may be one piece to the puzzle for explaining the high sensitivity for growth with the pulsed composition we observe in this work. Any deviations from an ideal composition may lead to etching through formation of volatile molybdenum oxochlorides.[29]

There is an obvious discrepancy between the composition measured by XRF and EDS. The EDS measurements suggest a significant over-stoichiometry of Ca for most samples. Re-measuring a sample that by EDS is measured to have 66% Ca versus (Mo + Ca) gives around 45% Ca by XRF. The XRF results are closer to the desired one to one stoichiometry between Ca and Mo. One difference between those measurement methods is the size of the volume being measured, where XRF measures the entire volume of the mounted sample and EDS is measuring a much more limited interaction volume.[37] In general, XRF is regarded to have a significantly higher precision[38] and we, therefore, believe that the over-stoichiometry of Ca may be less pronounced than suggested from the EDS data. The quantification of the EDS data may also suffer from the fact that the largest signal came from the Si-substrate since the electron penetration depth was longer than the film thickness.

The effect of annealing time on the crystallinity and photoluminescence were somewhat surprising, as annealing for 15 min yielded less luminescent films than not annealing at all or annealing for 30 min. Furthermore, the films became less XRD-crystalline with longer annealing times. This may be due to clustering of defects in the films or decomposition of the films leading to formation of $CaCO_3$ and reactions between Mo and the Si-substrate to form Mo-Si phases such as Mo_5Si_3.[39]

In general, the literature shows a huge divergence in annealing conditions for synthesis of $CaMoO_4$, ranging from heating the samples at 900 °C for 2 h[40] to 200 °C for 2 h.[27] The latter work also found that heating at 600 °C for 10 min is giving less luminescent films than heating at 200 °C for 2 h, which is contradicting our findings where 612.5 °C provides highly luminescent films. This divergence in published literature is yet another reason why CCD has been very useful here, as it allows for trying many combinations of annealing times and temperatures with few experiments.

The origin of the green luminescence at room temperature for Scheelite-structured molybdates is still disputed in the literature. It is suggested to stem from both oxygen deficient complexes,[41] defect centers with oxygen interstitials.[42] For the similar $CaWO_4$, it is suggested to stem from distorted WO_4-tetrahedra due to oxygen.[43] It is also more recently shown that more disorder leads to a higher luminescence at room temperature.[27] This is consistent with our findings visualized in Fig. 3—that even if the crystallinity is slightly decreased for the samples annealed for the longest times, the PL signal still increases significantly.

IV. SUMMARY AND CONCLUSIONS

A route for deposition of luminescent $CaMoO_4$ by ALD was successfully developed using a DoE-approach, using $MoCl_4O$, $Ca(thd)_2$, O_3, and H_2O as precursors. The optimization suggests that

depositing at 349 °C with 29% pulsed Mo and annealing at 626 °C for 30 min yields the most luminescent films. The growth is highly sensitive to the pulsed composition, and the actual run closest to the optimum used 29 pulsed % Mo at a deposition temperature of 350 °C, providing a growth rate of 1.2 Å/cycle. This work shows how DoE can be used to slash the number of required experiments to obtain a route for deposition of complex materials by ALD and provides a starting ground for further similar developments.

ACKNOWLEDGMENTS

REFERENCES

[1]M. Getz, P.-A. Hansen, M. A. K. Ahmed, H. Fjellvåg, and O. Nilsen, Dalton Trans. **46**, 3008 (2017).
[2]M. N. Getz, O. Nilsen, and P.-A. Hansen, Sci. Rep. **9**, 10247 (2019).
[3]J. E. Bratvold, H. H. Sønsteby, O. Nilsen, and H. Fjellvåg, J. Vac. Sci. Technol. A **37**, 021502 (2019).
[4]H. H. Sønsteby, H. Fjellvåg, and O. Nilsen, Adv. Mater. Interfaces **4**, 1600903 (2017).
[5]O. Nilsen, M. Lie, H. F. Fjellvåg, and A. Kjekshus, in *Growth of Oxides with Complex Stoichiometry by the ALD Technique, Exemplified by Growth of La$_{1-x}$Ca$_x$MnO$_3$, in Rare Earth Oxide Thin Films*, edited by M. Fanciulli and G. Scarel (Springer Berlin Heidelberg, Berlin, 2007), pp. 87–100.
[6]V. Czitrom, Am. Statistician **53**, 126 (1999).
[7]F. Yates, Biometrics **20**, 307 (1964).
[8]R. L. Plackett and J. P. Burman, Biometrika **33**, 305 (1946).
[9]N. R. Draper, in *Introduction to Box and Wilson (1951) on the Experimental Attainment of Optimum Conditions, in Breakthroughs in Statistics*, Springer Series in Statistics (Perspectives in Statistics), edited by S. Kotz and N. L. Johnson (Springer New York, New York, NY, 1992), pp. 267–269.
[10]G. Box and D. Behnken, Technometrics **2**, 455 (1960).
[11]S. R. Coles, D. K. Jacobs, J. O. Meredith, G. Barker, A. J. Clark, K. Kirwan, J. Stanger, and N. Tucker, Appl. Polym. Sci. **117**, 2251 (2010).
[12]A. Nourbakhsh, B. Ganjipour, M. Zahedifar, and E. Arzi, Nanotechnology **18**, 115715 (2007).
[13]F. Niamh Mac, Y. Ye, Q. Runzhang, G. Federico, and G. Stefan, e-print ChemRxiv (2019).
[14]D. M. King, X. Du, A. S. Cavanagh, and A. W. Weimer, Nanotechnology **19**, 445401 (2008).
[15]D. M. King, S. I. Johnson, J. Li, X. Du, X. Liang, and A. W. Weime, Nanotechnology **20**, 195401 (2009).
[16]M. Burke, A. Blake, I. M. Povey, M. Schmidt, N. Petkov, P. Carolan, and A. J. Quinn, J. Vac. Sci. Technol. A **32**, 031506 (2014).
[17]E. Cavalli, P. Boutinaud, R. Mahiou, M. Bettinelli, and P. Dorenbos, Inorg. Chem. **49**, 4916 (2010).
[18]E. Cavalli, P. Boutinaud, and M. Grinberg, J. Lumin. **169**, 450 (2016).
[19]P. Boutinaud, E. Pinel, M. Oubaha, R. Mahiou, E. Cavalli, and M. Bettinelli, Opt. Mater. **28**, 9 (2006).
[20]P. Boutinaud, R. Mahiou, E. Cavalli, and M. Bettinelli, J. Appl. Phys. **96**, 4923 (2004).
[21]P. Boutinaud, R. Mahiou, E. Cavalli, and M. Bettinelli, Chem. Phys. Lett. **418**, 185 (2006).
[22]P. Boutinaud, R. Mahiou, E. Cavalli, and M. Bettinelli, J. Lumin. **122–123**, 430 (2007).
[23]X. Li, Z. Yang, L. Guan, J. Guo, Y. Wang, and Q. Guo, J. Alloys Compd. **478**, 684 (2009).
[24]J. H. Ryu, J.-W. Yoon, C. S. Lim, W.-C. Oh, and K. B. Shim, J. Alloys Compd. **390**, 245 (2005).
[25]W. S. Cho, M. Yashima, M. Kakihana, A. Kudo, T. Sakata, and M. Yoshimura, J. Am. Ceram. Soc. **80**, 765 (1997).
[26]L. Zhu, Y. Mao, Q. Chen, Y. Zou, X. Shen, and G. Liao, J. Mater. Sci. Mater. Electron. **30**, 3639 (2019).
[27]A. P. de Azevedo Marques, V. M. Longo, D. M. A. de Melo, P. S. Pizani, E. R. Leite, J. A. Varela, and E. Longo, J. Solid State Chem. **181**, 1249 (2008).
[28]O. Nilsen, H. Fjellvåg, and A. Kjekshus, Thin Solid Films **450**, 240 (2004).
[29]J. N. Kvalvik, J. Borgersen, P.-A. Hansen, and O. Nilsen, J. Vac. Sci. Technol. A **38**, 042406 (2020).
[30]M. Putkonen and L. Niinistö, "Organometallic precursors for atomic layer deposition," in *Precursor Chemistry of Advanced Materials*, edited by R. A. Fischer (Springer Berlin Heidelberg, Berlin, 2005), pp. 125–145.
[31]A. Bertuch, G. Sundaram, M. Saly, D. Moser, and R. Kanjolia, J. Vac. Sci. Technol. A **32**, 01A119 (2014).
[32]K. Hinkelmann and O. Kempthorne, *Introduction to Experimental Design. Design and Analysis of Experiments* (John Wiley & Sons, Hoboken, NJ, 2008).
[33]G. S. Pawley, J. Appl. Crystallogr. **14**, 357 (1981).
[34]K. K. Sawant, V. P. Mundada, and V. J. Patel, J. Nanomed. Nanotechnol. **8**, 1000442 (2017).
[35]Á Kukovecz, D. Méhn, E. Nemes-Nagy, R. Szabó, and I. Kiricsi, Carbon **43**, 2842 (2005).
[36]B. Cao, L. A. Adutwum, A. O. Oliynyk, E. J. Luber, B. C. Olsen, A. Mar, and J. M. Buriak, ACS Nano **12**, 7434 (2018).
[37]J. I. Goldstein, D. E. Newbury, J. R. Michael, N. W. Ritchie, J. H. J. Scott, and D. C. Joy, *Scanning Electron Microscopy and X-ray Microanalysis* (Springer New York, New York, 2017), p. 12.
[38]G. R. Lachance and F. Claisse, *Quantitative X-ray Fluorescence Analysis Theory and Application* (John Wiley & Sons, Hoboken, NJ, 1995), p. 7.
[39]C. L. Fu, X. Wang, Y. Y. Ye, and K. M. Ho, Intermetallics **7**, 179 (1999).
[40]E. Cavalli, F. Angiuli, P. Boutinaud, and R. Mahiou, J. Solid State Chem. **185**, 136 (2012).
[41]E. V. Sokolenko, V. M. Zhukovskii, E. S. Buyanova, and Y. A. Krasnobaev, Inorg. Mater. **34**, 499 (1998).
[42]T. Hara, Mater. Chem. Phys. **91**, 243 (2005).
[43]B. M. Sinelkov, E. V. Sokolenko, and V. Y. Zvekov, Inorg. Mater. **32**, 999 (1996).
[44]See the supplementary material at https://doi.org/10.1116/6.0000327 for experimental setup and order, batching of ALD syntheses and annealing experiments, residuals vs experiment order and UV-VIS spectra of CaMoO4 on silica as deposited.